International Journal of Mass Spectrometry 308 (2011) 98–108

Contents lists available at ScienceDirect

International Journal of Mass Spectrometry

journal homepage: www.elsevier.com/locate/ijms

Tandem mass spectrometry studies of protonated and alkali metalated peptoids: Enhanced sequence coverage by metal cation addition

Kiran K. Morishetti[a], Scott C. Russell[b], Xiaoning Zhao[a], David B. Robinson[c], Jianhua Ren[a,*]

[a] Department of Chemistry, University of the Pacific, 3601 Pacific Avenue, Stockton, CA 95211, United States
[b] Department of Chemistry, California State University at Stanislaus, One University Circle, Turlock, CA 95382, United States
[c] Sandia National Laboratories, 7011 East Avenue, Livermore, CA 94550, United States

ARTICLE INFO

Article history:
Received 17 May 2011
Received in revised form 1 August 2011
Accepted 2 August 2011
Available online 10 August 2011

Keywords:
Peptoid
Peptide mimics
Alkali metal adducts
Lithium cation
Fragmentation
Collision induced dissociation

ABSTRACT

The fragmentation characteristics of five oligo-peptoids were studied under tandem mass spectrometry conditions. The charged peptoids were produced by protonation and alkali metal cation (Li^+, Na^+, K^+, Rb^+, and Cs^+) addition. The peptoids were ionized by the MALDI process and the resulting ions were fragmented via collision-induced dissociation (CID) experiments. All charged peptoids fragmented predominantly at the amide bonds. Highly abundant and sequence-dependent fragment ions were observed. The fragmentation patterns for the protonated peptoids and the metal cation adducts were strikingly different. All protonated peptoids fragmented by producing predominantly Y-type ions. The bias towards Y-ions was largely due to the greater proton affinity of the secondary amine at the terminal side of the Y-ions. All alkali metalated peptoids fragmented by producing both Y′- and B′-type ions, suggesting a "mobile metal cation" mechanism. For the peptoids with basic side chains, formation of the most abundant ions corresponded to the cleavage of the amide bonds at or near the basic residue. These results suggest that the metal cations are largely coordinated to the side chain of the basic residue. Chelation between the metal cation and the amino groups of the peptoids is an important factor to stabilize the fragment ions. For the peptoid without a basic side chain, the ion intensity was evenly distributed among all medium sized fragment ions. Fragmentations of protonated and alkali metalated peptoids yielded complementary sequential information, which demonstrated the practical utility of using mass spectrometry methods for *de novo* sequencing of peptoid libraries generated by combinatorial chemistry.

1. Introduction

Peptoids are peptidomimetic oligomers [1], best described as N-substituted polyglycines, such that the side chains are attached to the amide nitrogen rather than the α-carbon [2,3]. Peptoids can form peptide-like secondary structures. Studies using NMR, X-ray crystallography, and circular dichroism (CD) have shown that peptoids with N-α chiral aromatic side chains can fold into a polyproline type-I helix with a 3-fold periodicity [4–8]. Results from fluorescence resonance energy transfer (FRET) experiments suggest that peptoids with certain constructs can also form helix bundles [9]. The zinc metal cation has been shown to promote helix bundle formation for peptoids with thiol and imidazoles moieties [10].

Peptoids can easily be constructed via a solid-phase synthesis strategy that incorporates a two-step monomer addition cycle [11]. Hundreds of monomers with a wide variety of side-chains are available for peptoid synthesis. The efficient synthesis protocols, the diverse side chain functionalities, and the possible structural modulation have made peptoids an attractive platform for combinatorial libraries, bio-applications, and nanomaterials [12–14].

Peptoids have been considered as promising peptide-mimicking therapeutic agents. For example, unlike peptides, peptoids are resistant to protease digestion and have a high metabolic stability [15,16]. Due to a lack of NH groups in the backbone, peptoids have also shown enhanced membrane permeability [17–19]. A wide variety of biologically active peptoids and peptoid–peptide hybrids have been discovered. Some oligomer peptoids have been shown to bind to proteins and function as inhibitors or activators [20–23]. Peptoid mimics of antimicrobial peptides exhibit effective antibacterial activity [24,25]. Some helical peptoids could serve as lung surfactant mimetics [26,27]. Many biologically active peptoids have been discovered by screening large and diverse combinatorial peptoid libraries [28,29].

The rapidly growing number of studies on peptoids and the increasingly diverse structures in peptoid libraries require efficient analytical methods to analyze the sequences and the structural changes of peptoids. Direct sequencing of peptoids on the solid

* Corresponding author. Tel.: +1 209 946 2393; fax: +1 209 946 2607.
E-mail address: jren@pacific.edu (J. Ren).

1387-3806/$ – see front matter © 2011 Elsevier B.V. All rights reserved.
doi:10.1016/j.ijms.2011.08.003

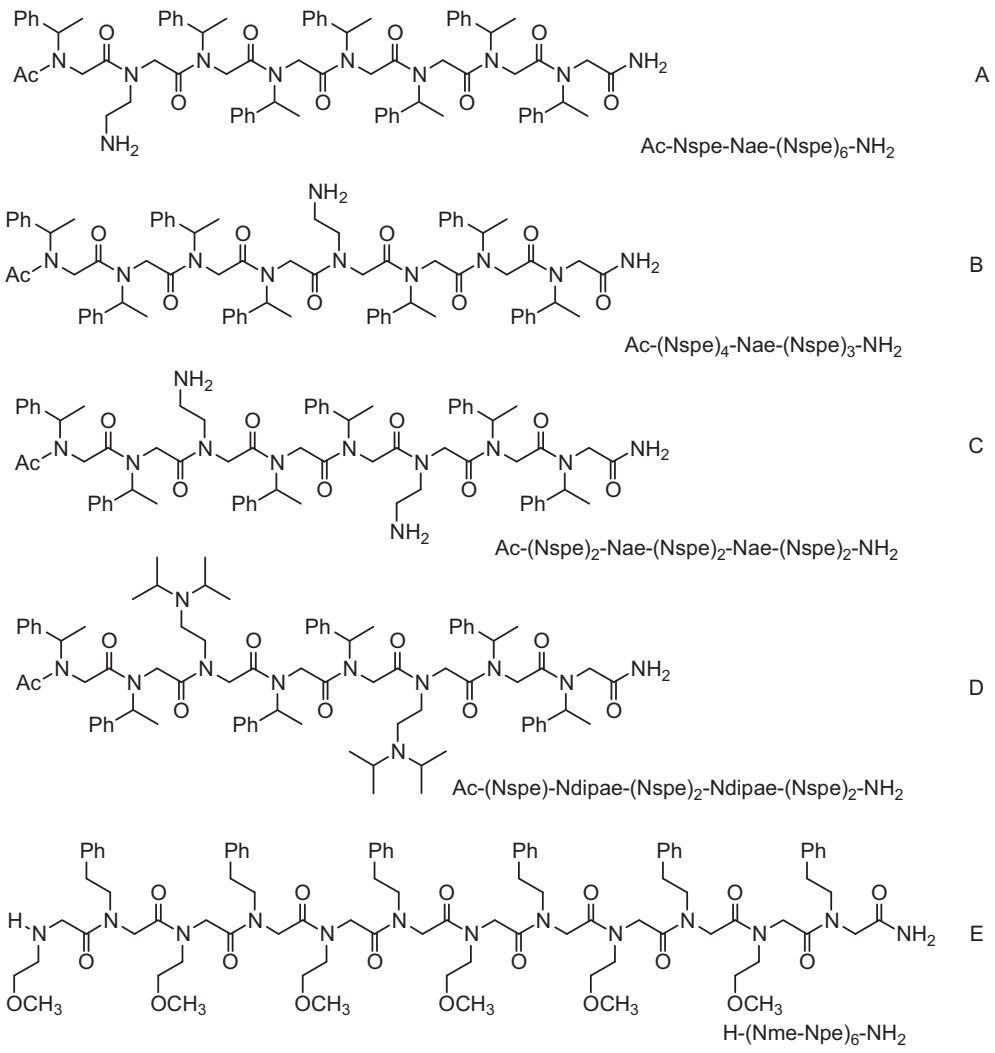

Scheme 1.

support resin by Edman degradation has been a common practice. However, this method is extremely time-consuming, since it requires the synthesis and analysis of standards for each unnatural residue [29–31]. Tandem mass spectrometry (MS/MS) is a well-established analytical method and it has been routinely used to characterize peptides and proteins [32,33]. Mass spectrometry techniques have also shown promise as the method of choice for analyzing the sequences and structures of peptoids [34–40]. Using fast atom bombardment (FAB) ionization combined with high-energy collision-induced dissociation (CID) as well as nano-electrospray ionization combined with low-energy CID, Liskamp and coworkers have studied the fragmentation patterns of oligopeptoids and peptoid–peptide hybrids [37,39,40]. They found that the protonated peptoids fragmented in a similar manner as those found in peptides. The predominant fragments correspond to dissociation at the amide bonds. In order to rapidly sequence the one-bead-one-compound peptoid library using tandem mass spectrometry techniques, Zuckermann and coworkers developed a method that allows an isotope tag containing bromine to be attached to the C-terminal end of the peptoids [35]. In MS/MS experiments, the ions that retain the C-termini (Y-type ions) could be easily recognized by their bromine isotope distribution. Pei and

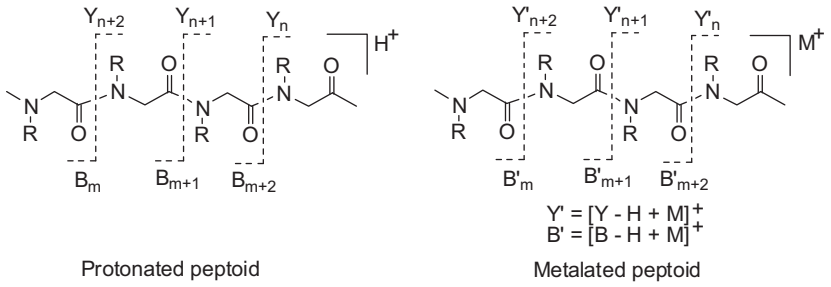

Scheme 2.

coworkers also developed a method that combines partial Edman degradation and mass spectrometry analysis for high-throughput sequencing of a peptoid library [34].

We recently studied a group of peptoids consisting of eight to twelve residues of N-substituted glycine using tandem mass spectrometry techniques. The peptoids were ionized by either protonation or alkali metal cation addition/adduct formation. We observed abundant sequence-dependent fragmentation ions from these peptoids. One striking observation was the significantly enhanced fragment ions from alkali metalated peptoids as compared to the protonated ones.

In this paper, we demonstrate this effect using a set of five peptoids shown in Scheme 1, that allow us to examine how the fragmentation patterns were influenced by the differences of the backbone structures, the locations of the basic side chains, as well as the type of the charge carrier (proton versus metal cations). Four of the peptoids, A–D, consisted mostly of residues with a bulky chiral aromatic side group, (*S*)-*N*-(1-phenylethyl) glycine (Nspe), that restricts the conformational freedom of the molecule. The N-terminus was acetylated, but one or two basic sites were introduced at varying positions. In peptoid-A, the second residue (from the N-terminus) was *N*-(2-aminoethyl)glycine (Nae) and in peptoid-B, the fifth residue was replaced by Nae. In peptoid-C, the third and the sixth residues were Nae. Peptoid-D was an analog of peptoid-C in which the smaller amino side groups were replaced by the bulky diisopropyl groups. Peptoid-E consisted of alternating *N*-(2-methoxyethyl)glycine (Nme) and *N*-(2-phenylethyl)glycine (Npe). These side groups were less bulky and anchiral, allowed greater conformational flexibility. A basic site was present at the N-terminus of peptoid-E as a secondary amine.

All these peptoids exhibited characteristic fragmentations under tandem mass spectrometry conditions. Alkali metalation showed the potential utility of sequencing peptoid library by mass spectrometry methods.

2. Experimental

2.1. Nomenclature

Under CID conditions, all charged peptoids, A–E, dissociated to yield sequence related fragment ions. Most of the fragment ions were formed by dissociation of the amide bonds of the peptoid backbone, which were similar to the formation of the y- and b-series of ions (the Roepfstorff nomenclature [41]) from the dissociation of the protonated peptides [42]. Similar peptoid fragmentation patterns have been observed earlier by Liskamp and coworkers [37,39,40]. In this paper, we have applied the Roepfstorff nomenclature to characterize the types of fragmentation ions from charged peptoids, Scheme 2.

2.2. Mass spectrometry measurements

The mass spectrometry (MS) and tandem mass spectrometry (MS/MS) experiments were carried out using a linear quadrupole ion trap coupled to a Fourier transform ion cyclotron resonance mass spectrometer, via a hybrid LTQ-FT (Thermo Finnigan, Bremen, Germany). The instrument was equipped with electrospray ionization (ESI) and atmospheric-pressure matrix-assisted laser desorption/ionization (AP-MALDI) (MassTech, Inc., Columbia, MD) sources. Some of the experiments were also performed using an LTQ mass spectrometer (Thermo Scientific, San Jose, CA) equipped with an AP-MALDI ion source (MassTech, Inc., Columbia, MD). Similar electronic conditions were applied for both instruments: plate voltage 1.8–3.2 kV, capillary temperature 200 °C, capillary voltage 46.0 V, and tube lens voltage 85.0 V. Ions were generated upon irradiation with a 337 nm ionizing nitrogen laser. The ions were isolated in the ion trap and subjected to collision-induced dissociation. The following conditions were used for the CID experiments, precursor ion isolation width 2–3 *m*/*z* units, normalized collision energy (NCE) 20–25%, activation Q 0.25, activation time 30 ms. Whenever possible, the same normalized CID energy was used in each case to enable comparisons of fragmentation characteristics of protonated peptoids and peptoid–metal adducts. All spectra were recorded in the profile mode using the normal scan speed.

The MALDI samples were prepared using the following procedure: 1 μL of peptoid samples ($\sim 10^{-5}$ M) were prepared in a 1:1 (v:v) mixture of MeOH:H_2O. For protonated ions, 1 μL of peptoid solution was spotted, followed immediately by 1 μL of matrix solution A (10 mg/mL) α-cyano-4-hydroxycinnamic acid (CHCA) in 70% acetonitrile (ACN), 0.1% trifluoroacetic acid (TFA) and allowed to air dry. For alkali metal adducts, 1 μL of peptoid solution was spotted, followed immediately by 1 μL of a 0.1 M solution of MCl (M = Li, Na, K, Rb, or Cs). This was immediately followed by the addition of 1 μL of matrix solution B (10 mg/mL CHCA in 70% ACN) and allowed to air dry. Water was purified using the Milli-Q system (Millipore, Billerica, MA). All other solvents and reagents were purchased from Sigma–Aldrich (St. Louis, MO).

2.3. Peptoid synthesis

Peptoids A–D were synthesized using the solid-phase synthesis strategy on Rink amide resin (EMD chemicals, Gibbstown, NJ). A slightly modified Aapptec Apex 396 synthesizer was employed for the synthesis [43]. In each step, the reaction vessel is agitated and then drained by suction filtration. 0.1 g resin was added to the reaction vessel and swollen for 1 min with dimethylformamide (DMF, Aldrich, St. Louis, MO) which was the solvent in all cases, except as noted. The Fmoc protecting group was removed by a 1-min and then 12-min treatment with 20% 4-methylpiperidine (Alfa, Ward Hill, MA). After thorough rinsing, the peptoid oligomer was synthesized through alternating acylation and nucleophilic displacement steps. In the acylation step, 1 mL of 1.2 M bromoacetic acid (Aldrich) was added, followed by 0.18 mL of neat diisopropylcarbodiimide (Advanced Chemtech, Louisville, KY) and reacted for 30 min, followed by rinsing. In the displacement step, 1 M of the primary amine was added and reacted for 100 min and then rinsed. The primary amines used included *N*-(2-aminoethyl) *t*-butyl carbamate (ae, Chem-Impex, Wood Dale, IL), diisopropylaminoethylamine (dipae, Fluka, St. Louis, MO), and (*S*)-1-phenylethylamine (spe, Acros, Pittsburgh, PA). In the latter case, *N*-methylpyrrolidone was used as the solvent, but DMF can also be used. A specific sequence of amines was added in displacement steps, interleaved with acylation steps. The peptoid was acetylated by adding a mixture of acetic anhydride and pyridine (both at 0.4 M) and allowed to react for 2 h, followed by rinsing with DMF. The resin was removed into a glass flask and products were cleaved from the resin by adding 4 mL of 95% trifluoroacetic acid/5% water and agitating for 5 min, followed by evaporation of the solvent. The Rink amide resin results in a primary amide at the C-terminus upon cleavage. This step also removes *t*-butyl carbonate from the Nae sidegroup, leaving a primary amine. We observed that prolonged cleavage times could result in the loss of a terminal fragment when the N-terminus is acetylated Nspe. The dry product was dissolved in a mixed solvent of water:acetonitrile (60:40, v:v) and passed through a 0.5 μm syringe filter to remove resin. The product was purified in four batches on a Vydac 10 mm, 22 mm × 250 mm C4 column using a 5–95% water–acetonitrile gradient, both with 0.1% trifluoroacetic acid. Fractions corresponding to the main peak or peaks were collected and analyzed by LC–MS with a similar gradient (Agilent 1100 series, LC/MSD Trap XCT, Vydac C4 column), concentrated by

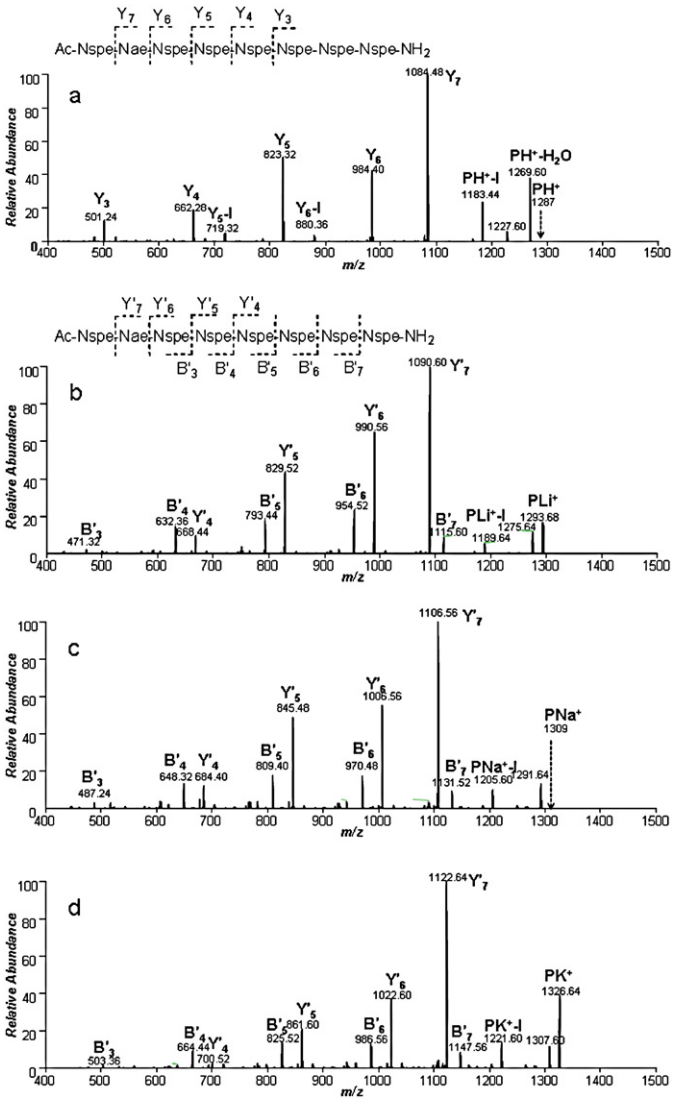

Fig. 1. CID spectra of peptoid-A with (a) H^+, (b) Li^+, (c) Na^+ and (d) K^+, where I = C_6H_5–CH=CH_2.

vacuum centrifugation, and lyophilized. Peptoid-E was provided by Dr. Ronald Zuckermann (LBNL).

3. Results

3.1. Peptoid-A

Peptoid-A was a polymer of Nspe with an Nae residue inserted at the second position from the N-terminus. The CID spectra resulting from the charged peptoid-A are shown in Fig. 1. The protonated peptoid-A (*m*/*z* 1287) yielded a spectrum of Y-series of ions from Y_3 to Y_7, Fig. 1a. The most abundant ion was Y_7 followed by Y_5 and Y_6. The ions smaller than Y_3 were not observed because of the low-mass cut-off of the ion trap. The ion at *m*/*z* 1269 was 18 mass units smaller than the protonated peptoid-A. The mass difference would correspond to the loss of a water molecule. The reason for the water loss was not initially obvious and a proposed mechanism is presented in the discussion section. The ion at *m*/*z* 1183 corresponded to a side chain loss, C_6H_5–CH=CH_2, from the protonated peptoid. The same side chain losses were also observed for the Y_6 and Y_5 ions, as reflected by the two minor peaks at *m*/*z* 880 and *m*/*z* 719, respectively. No observable B-series of ions appeared in the spectrum.

The CID spectrum of lithiated peptoid-A (*m*/*z* 1293) is shown in Fig. 1b, which is strikingly different from that of the protonated one. Both the Y′- and the B′-series of ions were observed. The ion abundance pattern of the Y′-ions was similar to that of the protonated peptoid, where Y'_7 was the most intense ion followed by Y'_6 and Y'_5. For the B′-series of ions, from B'_4 to B'_7, the intensities were similar and were relatively lower than those of the Y′-ions. In addition to the Y′- and B′-ions, two other ions were observed at higher mass. The ion at *m*/*z* 1189 corresponded to the loss of C_6H_5–CH=CH_2 from the lithiated peptoid. The ion at *m*/*z* 1275 was 18 mass units smaller than the lithiated peptoid (*m*/*z* 1293), which corresponded to the loss of H_2O.

The CID spectrum of the sodiated peptoid-A (*m*/*z* 1309) is shown in Fig. 1c. This spectrum was almost identical to that of the lithiated one, except that all peaks were shifted by the difference in mass between Na and Li. Both the Y′- and the B′-series of ions were observed with Y'_7 as the most abundant ion followed by Y'_6 and Y'_5. The intensities of the B′-ions were all similar and were weaker than those of the Y′-ions. The two ions corresponding to the side chain loss (C_6H_5–CH=CH_2) at *m*/*z* 1205 and water loss at *m*/*z* 1291 were also observed in the CID spectrum.

The CID spectrum of the potassiated peptoid-A (*m*/*z* 1326) is shown in Fig. 1d. This spectrum qualitatively resembled that of the sodiated peptoid. Both the Y′- and the B′-series of ions were observed with Y'_7 as the most abundant ion. An ion corresponding to water loss at *m*/*z* 1307 was observed as well. A slight difference was that the relative intensity of Y'_7 was more pronounced than other fragment ions from the potassiated peptoid. The CID spectrum of the cesiated peptoid-A (Fig. S1, supplemental information) had the fragmentation features of all other peptoid-A metal adducts. Both Y′- and B′-ions were observed and Y'_7 was the most abundant fragment ion. The main difference for the cesiated peptoid was the enhancement of secondary fragmentations, most of which corresponded to the side chain (C_6H_5–CH=CH_2) loss from the corresponding B′-ions.

3.2. Peptoid-B

Peptoid-B had the same residue composition as peptoid-A. The only difference with peptoid-B was that the Nae residue was located in the middle of the peptoid chain. The CID spectra of protonated, lithiated and sodiated peptoid-B are shown in Fig. 2. The corresponding CID spectra of the K^+ and Cs^+ adducts of peptoid-B are available in the supplemental information (Fig. S2). In the CID spectrum (Fig. 2a) of the protonated peptoid-B (*m*/*z* 1288), only the Y-series of ions were observed. The Y_7 fragment ion was significantly more abundant than the rest of the ions. The peak at *m*/*z* 1183 corresponded to the loss of the side chain (C_6H_5–CH=CH_2) from the protonated peptoid.

The fragmentation pattern of the lithiated peptoid-B (*m*/*z* 1293) was dramatically different from that of the protonated peptoid. Both Y′- and B′-series of ions were observed in the CID spectrum (Fig. 2b). For the Y′-series of ions, the intensity plateau shifted to the lower mass region. The Y'_4 ion was the most abundant Y′-ion followed by Y'_6, Y'_5 and Y'_7. Overall, the intensities of the B′-type ions were weaker than the Y′-type ions. However, the intensity of B'_4 was unexpectedly dominant, and represented the most abundant ion in the CID spectrum.

The general features of the CID spectrum of the sodiated peptoid-B (*m*/*z* 1309, Fig. 2c) were similar to those of the lithiated peptoid. Both of the Y′- and B′-series of ions were observed and the intensities were centered around the medium sized ions. The abundances of the Y'_6, Y'_5 and Y'_4 ions were about the same with a

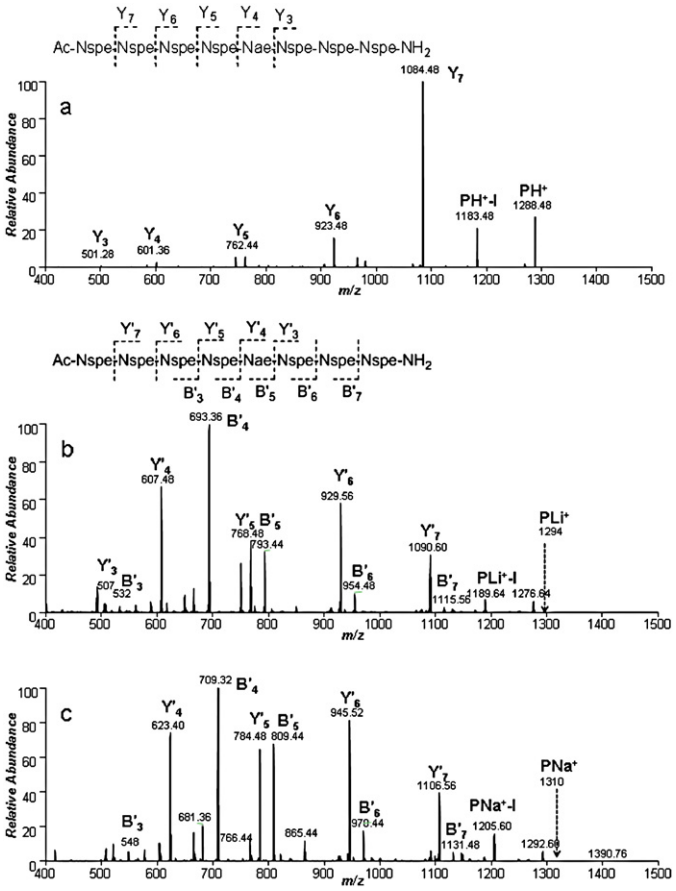

Fig. 2. CID spectra of peptoid-B with (a) H^+, (b) Li^+ and (c) Na^+, where I = C_6H_5–CH=CH_2.

slight increase for Y'_6. The B'_4 ion was still the most abundant ion in the spectrum, while B'_5 was also quite intense.

The CID spectrum of the potassiated peptoid-B (Fig. S2a) was qualitatively similar to those of the lithiated and sodiated peptoid-B with both Y′- and B′-series of ions observed in the spectrum. However, the relative ion intensities were different, while the intensity of B'_4 remained the strongest in the spectrum. The ion abundances of Y'_4 and Y'_5 reduced notably, while Y'_6 became as intense as B'_4. The CID spectrum of cesiated peptoid-B (Fig. S2b) qualitatively resembled that of the potassiated one. A slight difference was that the relative intensity of Y'_6 was reduced and B'_4 remained the most abundant ion in the spectrum.

3.3. Peptoid-C

Peptoid-C was a polymer of Nspe with two Nae residues placed at the third and the sixth positions from the N-terminus. The CID spectrum of protonated peptoid-C (*m*/*z* 1226) is shown in Fig. 3a. Only the Y-series of ions were observed and Y_7 was the most abundant ion. Interestingly, all of the Y-ions and the protonated peptoid ion were accompanied by an ion of 18 mass units smaller, which suggested a water loss from the corresponding precursor ion. The intensities of these companion ions were relatively strong. In fact, the companion ion (*m*/*z* 1208) of the protonated peptoid was the most abundant ion in the spectrum. In order to verify the observed masses of these companion ions, parallel experiments were performed by changing the ionization process and using different instrument conditions. Peptoid-C was ionized by both AP-MALDI and ESI process and the CID experiments were performed using the LTQ as well as the LTQ-FT instrument. Both experiments

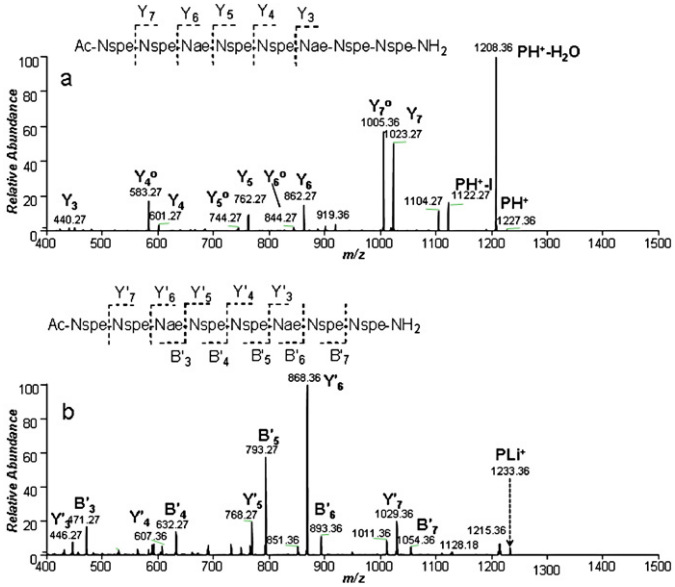

Fig. 3. CID spectra of peptoid-C with (a) H^+ and (b) Li^+, where I = C_6H_5–CH=CH_2 and $Y_n{}^o = Y_n - H_2O$.

produced the same results. The AP-MALDI data is shown in Fig. 3a and the ESI data is shown in Fig. S3aa.

The CID spectrum of the lithiated peptoid-C (*m*/*z* 1232) is shown in Fig. 3b. In addition to the Y′-series of ions, the B′-series of ions were observed. The most abundant ion in the spectrum was Y'_6. The B'_5 ion was the second most abundant fragment in the spectrum and was the most intense ion in the B′-series. Interestingly, most of the Y′-ions were also accompanied with a peak corresponding to a water loss.

The CID spectra of the Na^+, K^+, Rb^+ and Cs^+ adducts of peptoid-C are presented in Fig. S3. The ion abundance patterns were all similar to that of the lithiated peptoid. The only difference was the slightly reduced B'_5 ion intensity, which made the abundance of Y'_6 appear more pronounced.

3.4. Peptoid-D

The structure of peptoid-D resembled that of peptoid-C. The only difference was that the two Nae residues are replaced with two Ndipae. The CID spectra of protonated and lithiated peptoid-D are shown in Fig. 4 and the CID spectra of the other alkali metal adducts are presented in Fig. S4. The fragmentation patterns of peptoid-D almost mirrored those of peptoid-C, except that the peaks corresponding to 18 mass unit losses were absent for peptoid-D. For protonated peptoid-D (*m*/*z* 1395, Fig. 4a), only the Y-series of ions were observed and the most abundant ion was Y_7. The two peaks at *m*/*z* 1293 and *m*/*z* 1290 corresponded to the side chains losses of $(CH_3)_2CH$–NH–$CH(CH_3)_2$ and C_6H_5–CH=CH_2, respectively. For lithiated peptoid-D (*m*/*z* 1401, Fig. 4b), the most abundant ion shifted to Y'_6. The B′-series of ions were also observed with the intensity centered at B'_5. The CID spectra of other alkali (Na^+, K^+, Rb^+ and Cs^+) adducts of peptoid-D (Fig. S4) were all similar to that of the lithiated one.

3.5. Peptoid-E

Peptoid-E had 12 residues with alternating Nme and Npe monomers and did not have any basic side chain. The N-terminus was a secondary amine and is presumably the most basic site. The CID spectra of protonated, lithiated and sodiated peptoid-E are shown in Fig. 5 and the CID spectra of potassiated and cesiated

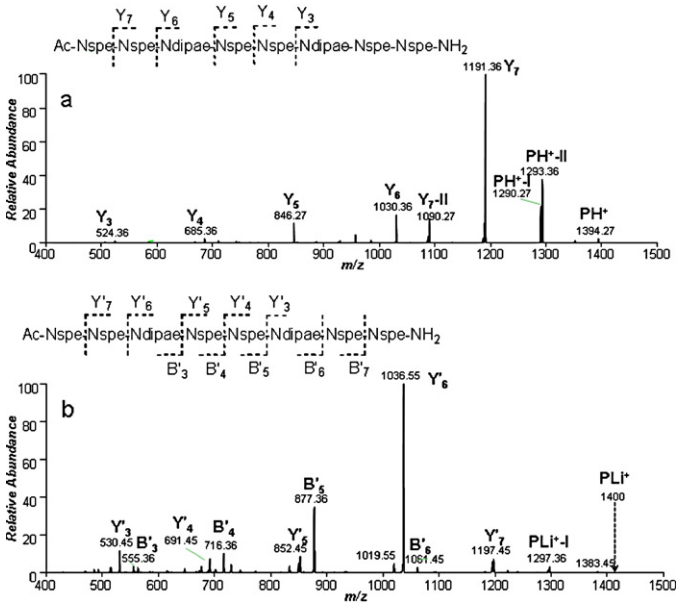

Fig. 4. CID spectra of peptoid-D with (a) H^+ and (b) Li^+, where I = C_6H_5–CH=CH_2 and II = $(CH_3)_2$CH–NH–CH$(CH_3)_2$.

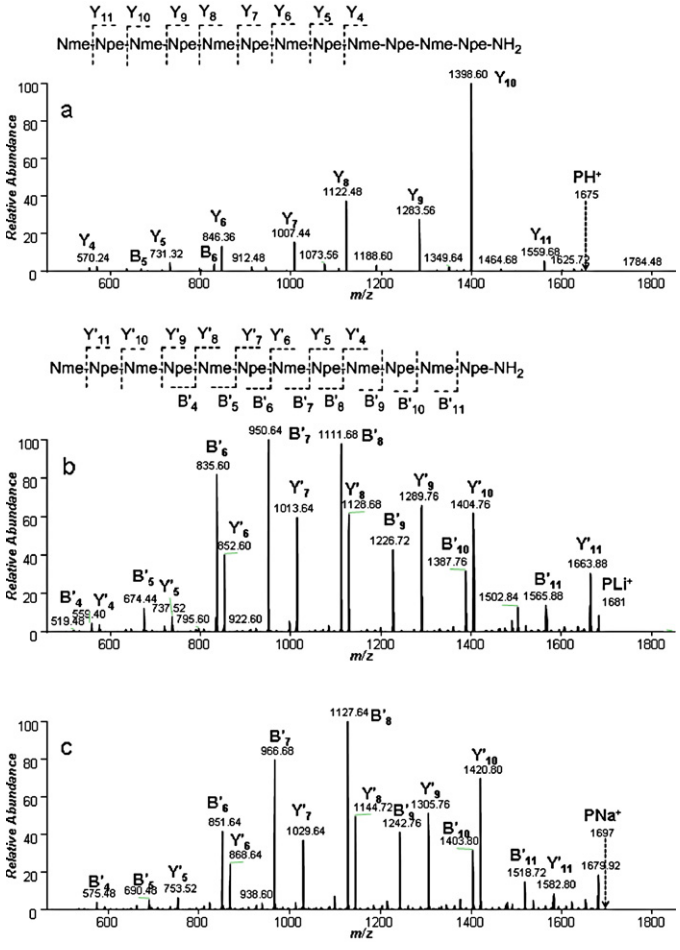

Fig. 5. CID spectra of peptoid-E with (a) H^+, (b) Li^+ and (c) Na^+.

peptoid-E are presented in Fig. S5. The protonated peptoid-E (*m*/*z* 1675) yielded a full spectrum of Y-series of ions upon performing CID with Y_{10} being the most abundant ion (Fig. 5a). Several B-ions appeared in the spectrum, but with very low abundances.

Upon CID, the lithiated peptoid-E (*m*/*z* 1681) produced a full spectrum of both Y′- and B′-series of fragment ions with relatively even distributions of ion intensities from Y'_6 to Y'_{10} and from B'_6 to B'_8 (Fig. 5b). The B′-ions were more abundant than the Y′-ions. The CID spectrum of sodiated peptoid-E (*m*/*z* 1697, Fig. 5c) showed features similar to those observed in the lithiated peptoid with slightly modified ion intensities. In the Y′-series of ions, the most intense peak was Y'_{10}. The intensity decreased gradually from Y'_9 to Y'_6. In the B′-series of ions, the intensity plateau was centered at B'_8. The intensities of $B'_{6,7}$ and $B'_{9,10}$ were relatively weaker. The potassiated peptoid-E had a similar fragmentation pattern to that of the sodiated species (Fig. S5a). In the Y′-series, the most abundant ion was Y'_{10} and the intensity decreased gradually from Y'_9 to Y'_6. In the B′-series of ions, the intensity plateau centered at the B'_8 ion. The fragmentation pattern of the cesiated peptoid-E was very similar to that of potassiated peptoid-E (Fig. S5b).

4. Discussion

Under CID conditions, all protonated peptoids (A–E) yielded nearly exclusively the Y-type of fragment ions with the most abundant ion centered at the largest Y-ion (the second of the largest Y-ion for peptoid-E). However, the alkali cationized peptoids (A–E) produced CID spectra in which both the Y′- and the B′-series of ions were of high intensities. For each of the peptoids, the fragmentation patterns associated with different alkali metal cations were similar. The most intense fragment ions tended to be centered at the medium mass ions and the ion intensities were sensitive to the locations of the basic residues in the peptoids. Most fragments from peptoid-C were accompanied by ions that were 18 mass units lower. Alkali metallated peptoid-E fragmented efficiently, yielding nearly equal intensities of all medium to larger mass ions.

4.1. Protonated peptoids

The fragmentation patterns of the protonated peptoids appeared quite different from those observed for most tryptic protonated peptides. For protonated peptides without terminal modifications and without basic side chains, the predominant fragments are often the b-type ions. The preference for the formation of b-type fragment ions has also been observed in peptides with N-terminal acetylation and C-terminal esterification [44]. For peptides with a basic residue (*e.g.*, lysine or arginine), the major fragments have been shown to vary depending on the location of the basic residue [45,46]. In the “mobile proton model”, upon collision, the proton(s) move to various protonation sites and induce fragmentation [47,48]. This model has been successfully used to describe the fragmentation mechanisms of various protonated peptides [33].

The “mobile proton model” may also be used to explain the fragmentation patterns of the protonated peptoids. The CID spectra of all five peptoids showed a similar characteristic that all Y-ions were formed and the larger ions were favored regardless of the basic residue locations. It is speculated that initially the proton is likely attached to the side chain amino group (peptoids A–D), or the N-terminal amino group (peptoid-E), or even an amide group. Upon collision, the proton moves to various amide bonds and induces fragmentation. The preference for the formation of the Y-ions is largely due to the enhanced basicity of the tertiary amide nitrogens in peptoids compared to the secondary amide nitrogens in peptides. Upon fragmentation, peptoids can form Y-ions with a

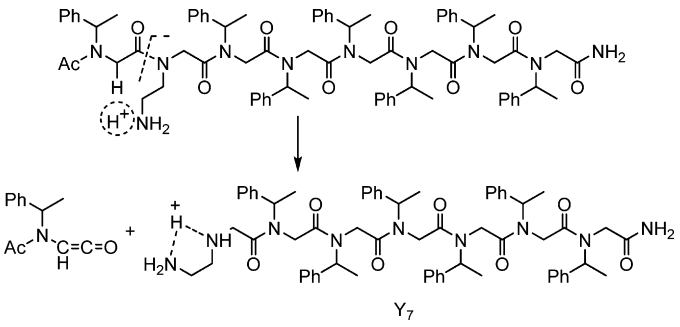

Scheme 3.

secondary amine at the terminal side, while peptides produce a primary amine. The preference for the formation of Y-type ions has also been observed for other peptoids by Liskamp and coworkers [37].

The Y_7 ion was the most intense fragment for all four peptoids, A–D. Peptoids A–D were all acetylated at the N-termini and all had eight residues. Formation of Y_7 corresponded to the cleavage at the first amide bond from the N-terminus. For peptoid-A, the cleavage occurred at the amide bond on the N-terminal side of the Nae residue, Scheme 3, where the dashed circle indicates the "mobile proton". It is thought that the resulting Y_7 ion can be stabilized by intramolecular H-bonding between the two amino groups at the N-terminus. The lost neutral molecule has a ketene structure (–CH=C=O). While peptoids C and D would form corresponding Y_7 ions with H-bonds at the N-terminus, the Y_7 ion produced from peptoid-B would not benefit from the similar H-bonding unless the backbone could bend such that the Nae side chain and the N-terminus are close enough to form a H-bond. Nonetheless the facile loss of the small ketene-like neutral molecule is likely the driving force for the formation of the Y_7 ions.

Peptoid-E did not have a basic side chain and the N-terminus was a free secondary amine. One would expect a balanced distribution between the Y- and B-ions. Interestingly, the predominantly

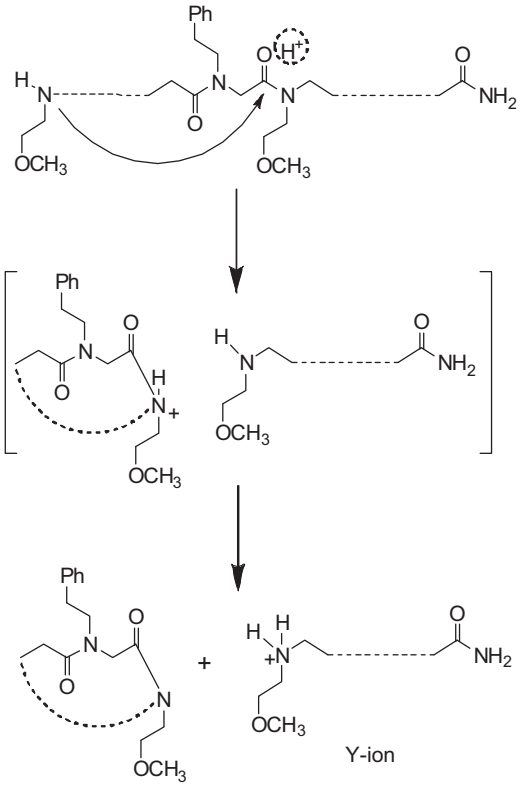

Scheme 4.

observed fragments were Y-ions as well. This may be explained by the "diketopiperazine pathway", Scheme 4, where the dash circle indicates the "mobile proton". The original "diketopiperazine pathway" was proposed to explain the formation of y_n-ions from protonated peptides [33]. In this mechanism, addition–elimination

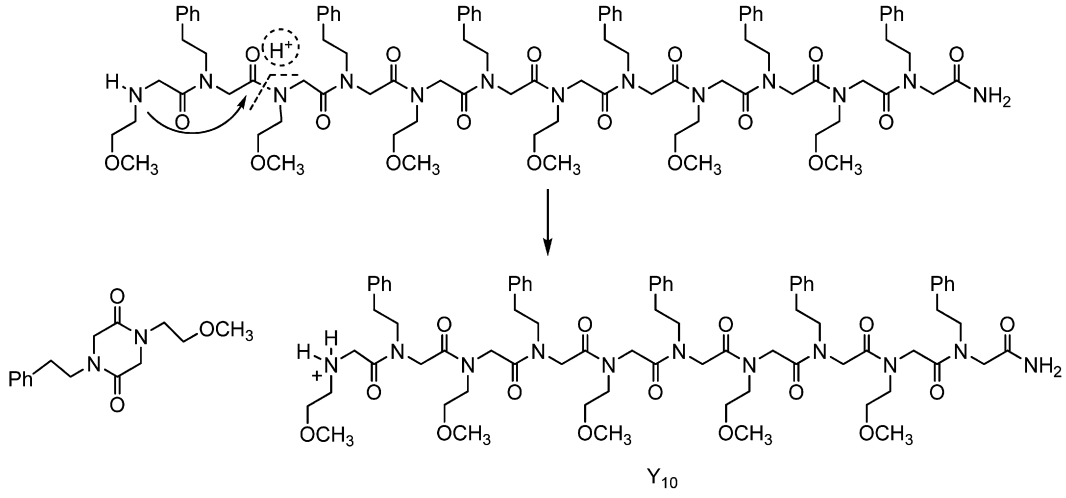

Scheme 5.

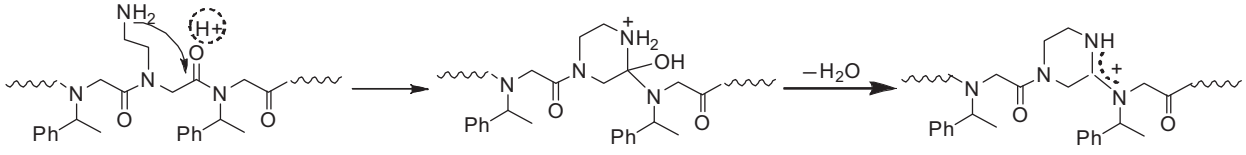

Scheme 6.

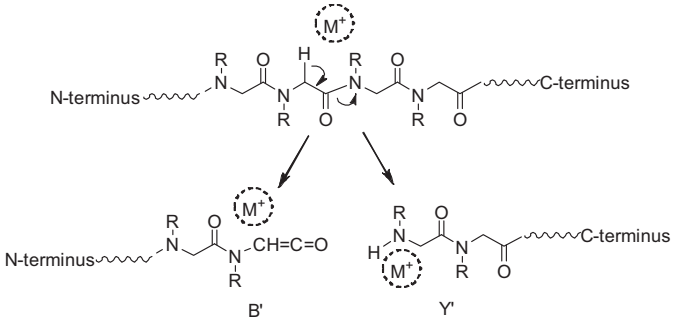

Scheme 7.

occurs between the N-terminal amine nitrogen and the protonated amide bond. This results in a cyclic structure and the N-terminal nitrogen becomes the newly formed amide nitrogen. The eliminated group is a secondary amine, which is more basic than an amide. The proton from the amide bond moves to the eliminated amine and forms the Y-ion. Y_{10} is the most intense fragment ion (Fig. 5a). Formation of Y_{10} corresponds to the cleavage at the second amide bond from the N-terminus. This would yield a neutral diketopiperazine, Scheme 5.

The protonated peptoid-C exhibited a facile neutral loss of 18 mass units, which corresponds to a water molecule. Interestingly, all Y-ions of peptoid-C were also accompanied by an ion of 18 mass units smaller (Fig. 3a). This peptoid did not have a carboxyl or a hydroxyl group that could promote water loss. Results from previous studies on peptides with N-terminal glutamine have shown that the protonated peptides did dissociate via water loss and form the intermediate structures involving a resonance stabilized 5-membered ring [49]. A similar mechanism may be used to explain the water loss in protonated peptoid-C and the proposed mechanism is shown in Scheme 6. The side chain amino group attacks the activated amide carbonyl group (by protonation) and forms a six-membered ring intermediate. By eliminating a water molecule, a resonance stabilized ion is formed. The same mechanism may be used to explain the water loss process from other peptoids. However, in peptoid-D, no such mass loss was observed. The basic side groups in this case were bulky tertiary amines that could not undergo this reaction, but that experiment added evidence that the water loss involved the amine side chains in the other peptoids.

4.2. Alkali metalated peptoids

The fragmentation patterns of the alkali metalated peptoids appeared significantly different from those observed from CID experiments of most alkali metal cationized peptides. Earlier studies have shown that the fragmentation spectra of alkali-cationized peptides were characterized by single amino acid losses from the C-terminus that were generally observed in the form of $[b_n+OH+M]^+$ [50,51]. A recent study suggested that alkali-cationized non-tryptic peptides tend to yield predominant y-type fragments, $[y_n+M]^+$ [45]. The same fragmentation pattern has also been shown in sodiated peptides with modified N- and C-termini [52]. It has been demonstrated that peptide fragmentation differs between protonated peptides and alkali metal adducts [45,46,50,52–55]. Unlike the highly mobile proton, alkali metal interactions with peptides seem to be localized. However, a general consensus on the site of localization of the metal ion appears unclear. It has been reported that the metal ion may bind to amide carbonyl oxygens [56–58], the C-terminus [54,59], amide nitrogens [55,60], side chain

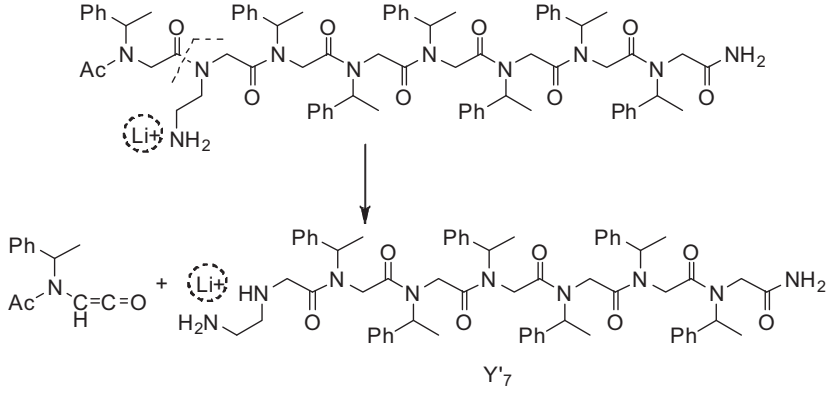

Scheme 8.

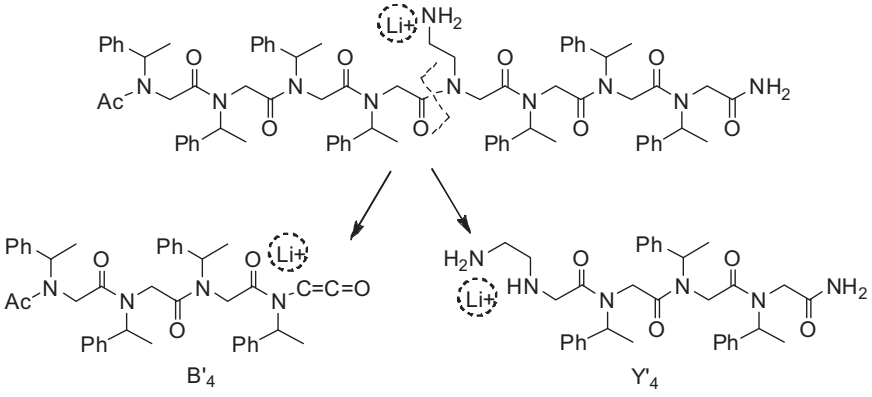

Scheme 9.

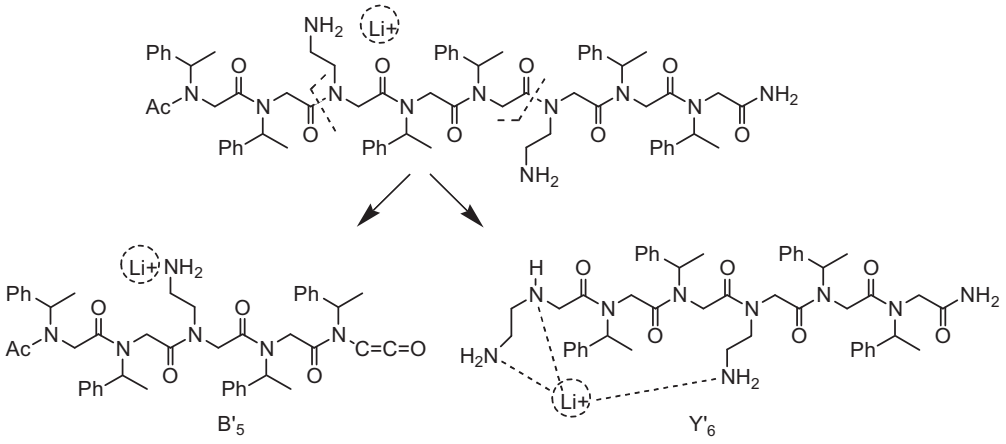

Scheme 10.

nitrogen(s), and the N-terminus [53], or a combination of these [61,62]. In addition, chelation and salt-bridge formation between peptide backbones/termini and alkali metal ions may play important roles [63–65]. For helical peptides, the favored site of metallation is likely the C-terminus and the fragmentation pattern of the metalated peptides seem to reflect this feature [66,67]. However, a recent study on doubly charged peptides, $[peptide+H+M]^{2+}$, showed that the b-ions tend to be alkali metal cationized while the y-ions are protonated, suggesting the location of the metal cation towards the peptide N-terminus [46].

All five alkali metalated peptoids (A–E) produced both the Y′- and the B′-series ions. Regardless of the binding sites of the alkali metal cation, the fragmentation may be induced by a "mobile metal cation". A general fragmentation mechanism is shown in Scheme 7, where the dashed circle indicates the "mobile metal cation", and the curved arrow indicates the movement of the bonding electron pairs. Upon cleavage of an amide bond, a proton from the C–H bond transfers to the nitrogen atom, resulting in a ketene-like structure on the N-terminal side and a secondary amine on the C-terminal side. If the M^+ complexes to the C-terminal side, a Y′ ion is formed, and if the M^+ complexes to the N-terminal side, a B′ ion is formed.

Peptoids A and B were isomers with the basic residue Nae located at the second and fifth position, respectively. The CID spectra of metalated A and B were quite different. For peptoid-A, the intensities were centered at larger mass Y′ ions, while for peptoid-B, the intensity plateau was around the medium mass Y′ and B′ ions. It seems that the preferred cleavage site was adjacent to the basic Nae residue. Y'_7 was the most abundant ion for peptoid-A with all akali metal cations. Formation of Y'_7 from peptoid-A corresponded to the cleavage at the N-terminal side of the Nae residue, Scheme 8. In Y'_7, the Li^+ was likely chelated with the two amino groups at the N-terminus. For the lithiated peptoid-B, the Y'_4 and B'_4 fragment ions were the most intense. Cleavage at the amide bond N-terminal side of the Nae residue would yield both B'_4 and Y'_4 (Scheme 9). In Y'_4, the Li^+ was likely chelated around the N-terminal amino groups, while in B'_4, the location of the lithium cation was unclear. The reason for the higher intensity of B'_4 over Y'_4 is not apparent. Compared to the lithiated peptoid-B, the spectrum of the sodiated peptoid-B featured enhanced intensities of B'_5 and $Y'_{5–6}$. In fact, the $B'_{4,5}$ and $Y'_{4–6}$ were about the same intensity. The proposed structures of these ions are shown in the supplemental information (Scheme S9).

Peptoid-C had two basic Nae residues. The CID spectrum of the lithiated peptoid-C exhibited two major fragment ions, Y'_6 and B'_5. These two ions were formed from the cleavage of the amide bonds on the N-terminal side of both the Nae residues (Scheme 10). It is thought that the Li^+ was likely chelated to the amino groups in both ions. The Y'_6 ion remained the most intense fragment in all other alkalated peptoid-C (Na^+, K^+, and Cs^+), while the B'_5 ion became weaker with increasing metal cation radius. The favored formation of the Y'_6 ion may be due to the strong chelation between the metal cation and the three amino groups. The same feature was observed in the metalated peptoid-D, an analog of peptoid-C. The Y'_6 ion was the most abundant fragment for all alkali metalated ions of peptoid-D.

The lithiated peptoid-E produced nearly even distributions of both Y′- and B′-series ions from B'_6 to B'_{10} and from Y'_6 to Y'_{10}. Similar fragmentation features appeared in all other alkali metal adducts of peptoid-E. The abundant fragmentation can be easily explained by the "mobile alkali metal cation" mechanism. Peptoid-E did not have a basic side chain, and the metal cation was likely initially coordinated to the N-terminal amino group. Upon CID, the metal ion could move along the peptoid backbone and induce fragmentation at various amide bonds. Statistically, the metal ion would have more chances of residing in the middle than at the ends of the peptoid, which explains the observed preference for middle mass fragment ions when a basic side chain is absent.

5. Conclusions

The fragmentation characteristics of five positively charged peptoids have been studied via collision induced dissociation experiments. All peptoids predominantly cleaved at the amide bonds. The fragmentation patterns for the protonated and the alkali metalated peptoids differed greatly. All protonated peptoids fragmented by producing predominantly Y-type ions, with the abundant fragments centered on higher mass ions. The bias towards Y-ions was largely due to the greater proton affinity of the secondary amine at the N-terminal side of the Y-ions. A diketopiperazine-like intermediate was postulated as being responsible for the preferred Y-ions in peptoids without N-terminal acetylation, such as peptoid-E. The alkali metal adducts of all peptoids fragmented by producing the full spectrum of both Y′-ions and B′-ions, which suggested a "mobile metal cation" induced fragmentation mechanism. For the peptoids with basic side chains (A–D), the formation of the most abundant ions corresponded to the fragmentation of the amide bonds at or near the basic residue, Nae. These results suggested that the metal cations were largely coordinated to the side chain of the Nae residue. Chelation between the metal ion and the amino groups of the peptoids was speculated to be an important factor in stabilizing the fragment ions. For the peptoid without a basic side chain (peptoid-E), the fragment ion intensities were distributed among all medium mass ions, further supporting the "mobile metal cation" mechanism. It is also

possible that a heterogeneous population of different metalated isomers was already formed during the ion formation process in the ion source. Fragmentations of protonated and alkali metallated peptoids provided complementary sequential information. Alkali metal cations induced broader sequence coverage of all peptoids studied. All five alkali metal cations (Li^+, Na^+, K^+, Rb^+ and Cs^+) had comparable influences on the fragmentation patterns. Protonation and metal cation addition, especially lithiation, thus provide practical utility in mass spectrometry methods for *de novo* sequencing of peptoid libraries generated by combinatorial chemistry.

Acknowledgements

The authors would like to thank Dr. Bogdan Bogdanov (University of Louisville, currently at the University of the Pacific) for assisting in the LTQ-FTICR experiments and Dr. Ronald Zuckermann (The Molecular Foundry, Lawrence Berkeley National Laboratory) for providing peptoid-E. J. Ren acknowledges the supports from the National Science Foundation (CHE-0749737) and the American Chemical Society Peptroleum Research Fund (Type-G). D. Robinson acknowledges the support from the Laboratory-Directed Research and Development program at Sandia National Laboratories (DE-AC04-94AL85000). Peptoid synthesis at the Molecular Foundry was supported by the Office of Science, Office of Basic Energy Sciences, US Department of Energy (DE-AC02-05CH11231).

Appendix A. Supplementary data

Supplementary data associated with this article can be found, in the online version, at doi:10.1016/j.ijms.2011.08.003.

References

[1] D.J. Hill, M.J. Mio, R.B. Prince, T.S. Hughes, J.S. Moore, A field guide to foldamers, Chem. Rev. 101 (2001) 3893–4011.
[2] R.J. Simon, R.S. Kania, R.N. Zuckermann, V.D. Huebner, D.A. Jewell, S. Banville, S. Ng, L. Wang, S. Rosenberg, C.K. Marlowe, D.C. Spellmeyer, R. Tans, A.D. Frankel, D.V. Santi, F.E. Cohen, P.A. Bartlett, Peptoids: a modular approach to drug discovery, Proc. Natl. Acad. Sci. U. S. A. 89 (1992) 9367–9371.
[3] P.S. Farmer, E.J. Ariens, Speculations on the design of nonpeptidic peptidomimetics, Trends Pharmacol. Sci. 3 (1982) 362–365.
[4] T.S. Burkoth, E. Beausoleil, S. Kaur, D. Tang, F.E. Cohen, R.N. Zuckermann, Toward the synthesis of artificial proteins. The discovery of an amphiphilic helical peptoid assembly, Chem. Biol. 9 (2002) 647–654.
[5] K. Kirshenbaum, A.E. Barron, R.A. Goldsmith, P. Armand, E.K. Bradley, K.T.V. Truong, K.A. Dill, F.E. Cohen, R.N. Zuckermann, Sequence-specific polypeptoids: a diverse family of heteropolymers with stable secondary structure, Proc. Natl. Acad. Sci. U. S. A. 95 (1998) 4303–4308.
[6] C.W. Wu, T.J. Sanborn, K. Huang, R.N. Zuckermann, A.E. Barron, Peptoid oligomers with alpha-chiral, aromatic side chains: sequence requirements for the formation of stable peptoid helices, J. Am. Chem. Soc. 123 (2001) 6778–6784.
[7] C.W. Wu, T.J. Sanborn, R.N. Zuckermann, A.E. Barron, Peptoid oligomers with alpha-chiral, aromatic side chains: effects of chain length on secondary structure, J. Am. Chem. Soc. 123 (2001) 2958–2963.
[8] C.W. Wu, K. Kirshenbaum, T.J. Sanborn, J.A. Patch, K. Huang, K.A. Dill, R.N. Zuckermann, A.E. Barron, Structural and spectroscopic studies of peptoid oligomers with alpha-chiral aliphatic side chains, J. Am. Chem. Soc. 125 (2003) 13525–13530.
[9] B.-C. Lee, R.N. Zuckermann, K.A. Dill, Folding a nonbiological polymer into a compact multihelical structure, J Am. Chem. Soc. 127 (2005) 10999–11009.
[10] B.-C. Lee, T.K. Chu, K.A. Dill, R.N. Zuckermann, Biomimetic nanostructures: creating a high-affinity zinc-binding site in a folded nonbiological polymer, J. Am. Chem. Soc. 130 (2008) 8847–8855.
[11] R.N. Zuckermann, J.M. Kerr, S.B.H. Kent, W.H. Moos, Efficient method for the preparation of peptoids [oligo(*N*-substituted glycines)] by submonomer solid-phase synthesis, J. Am. Chem. Soc. 114 (1992) 10646–10647.
[12] B. Yoo, K. Kirshenbaum, Peptoid architectures: elaboration, actuation, and application, Curr. Opin. Chem. Biol. 12 (2008) 714–721.
[13] S.A. Fowler, H.E. Blackwell, Structure–function relationships in peptoids: recent advances toward deciphering the structural requirements for biological function, Org. Biomol. Chem. 7 (2009) 1508–1524.
[14] C.A. Olsen, Peptoid–peptide hybrid backbone architectures, ChemBioChem 11 (2010) 152–160.
[15] S.M. Miller, R.J. Simon, S. Ng, R.N. Zuckermann, J.M. Kerr, W.H. Moos, Comparison of the proteolytic susceptibilities of homologous L-amino acid, D-amino acid, and N-substituted glycine peptide and peptoid oligomers, Drug Dev. Res. 35 (1995) 20–32.
[16] S.M. Miller, R.J. Simon, S. Ng, R.N. Zuckermann, J.M. Kerr, W.H. Moos, Proteolytic studies of homologous peptide and N-substituted glycine peptoid oligomers, Bioorg. Med. Chem. Lett. 4 (1994) 2657–2662.
[17] P.A. Wender, D.J. Mitchell, K. Pattabiraman, E.T. Pelkey, L. Steinman, J.B. Rothbard, The design, synthesis, and evaluation of molecules that enable or enhance cellular uptake: peptoid molecular transporters, Proc. Natl. Acad. Sci. U. S. A. 97 (2000) 13003–13008.
[18] Y.-U. Kwon, T. Kodadek, Quantitative evaluation of the relative cell permeability of peptoids and peptides, J. Am. Chem. Soc. 129 (2007) 1508–1509.
[19] N.C. Tan, P. Yu, Y.-U. Kwon, T. Kodadek, High-throughput evaluation of relative cell permeability between peptoids and peptides, Bioorg. Med. Chem. 16 (2008) 5853–5861.
[20] J.T. Nguyen, C.W. Turck, F.E. Cohen, R.N. Zuckermann, W.A. Lim, Exploiting the basis of proline recognition by SH3 and WW domains: design of N-substituted inhibitors, Science 282 (1998) 2088–2092.
[21] J.A.W. Kruijtzer, W.A.J. Nijenhuis, N. Wanders, W.H. Gispen, R.M.J. Liskamp, R.A.H. Adan, Peptoid–peptide hybrids as potent novel melanocortin receptor ligands, J. Med. Chem. 48 (2005) 4224–4230.
[22] B. Liu, P.G. Alluri, P. Yu, T. Kodadek, A potent transactivation domain mimic with activity in living cells, J. Am. Chem. Soc. 127 (2005) 8254–8255.
[23] R. Ruijtenbeek, J.A.W. Kruijtzer, W. Van de Wiel, M.J.E. Fischer, M. Fluck, F.A.M. Redegeld, R.M.J. Liskamp, F.P. Nijkamp, Peptoid–peptide hybrids that bind syk SH2 domains involved in signal transduction, ChemBioChem 2 (2001) 171–179.
[24] N.P. Chongsiriwatana, J.A. Patch, A.M. Czyzewski, M.T. Dohm, A. Ivankin, D. Gidalevitz, R.N. Zuckermann, A.E. Barron, Peptoids that mimic the structure, function, and mechanism of helical antimicrobial peptides, Proc. Natl. Acad. Sci. U. S. A. 105 (2008) 2794–2799.
[25] J.A. Patch, A.E. Barron, Helical peptoid mimics of magainin-2 amide, J. Am. Chem. Soc. 125 (2003) 12092–12093.
[26] S.L. Seurynck-Servoss, M.T. Dohm, A.E. Barron, Effects of including an N-terminal insertion region and arginine-mimetic side chains in helical peptoid analogues of lung surfactant protein B, Biochemistry 45 (2006) 11809–11818.
[27] N.J. Brown, C.W. Wu, S.L. Seurynck-Servoss, A.E. Barron, Effects of hydrophobic helix length and side chain chemistry on biomimicry in peptoid analogues of SP-C, Biochemistry 47 (2008) 1808–1818.
[28] R.N. Zuckermann, E.J. Martin, D.C. Spellmeyer, G.B. Stauber, K.R. Shoemaker, J.M. Kerr, G.M. Figliozzi, D.A. Goff, M.A. Siani, R. Simon, S.C. Banville, E.G. Brown, L. Wang, L.S. Richter, W.H. Moos, Discovery of nanomolar ligands for 7-transmembrane G-protein-coupled receptors from a diverse N-(substituted)glycine peptoid library, J. Med. Chem. 37 (1994) 2678–2685.
[29] P.G. Alluri, M.M. Reddy, K. Bachhawat-Sikder, H.J. Olivos, T. Kodadek, Isolation of protein ligands from large peptoid libraries, J. Am. Chem. Soc. 125 (2003) 13995–14004.
[30] D.G. Udugamasooriya, S.P. Dineen, R.A. Brekken, T. Kodadek, A peptoid "antibody surrogate" that antagonizes VEGF receptor 2 activity, J. Am. Chem. Soc. 130 (2008) 5744–5752.
[31] R. Liu, K.S. Lam, Automatic Edman microsequencing of peptides containing multiple unnatural amino acids, Anal. Biochem. 295 (2001) 9–16.
[32] R. Aebersold, M. Mann, Mass spectrometry-based proteomics, Nature 422 (2003) 198–207.
[33] B. Paizs, S. Suhai, Fragmentation pathways of protonated peptides, Mass Spectrom. Rev. 24 (2005) 508–548.
[34] A. Thakkar, A.S. Cohen, M.D. Connolly, R.N. Zuckermann, D. Pei, High-throughput sequencing of peptoids and peptide–peptoid hybrids by partial Edman degradation and mass spectrometry, J. Comb. Chem. 11 (2009) 294–302.
[35] M.G. Paulick, K.M. Hart, K.M. Brinner, M. Tjandra, D.H. Charych, R.N. Zuckermann, Cleavable hydrophilic linker for one-bead-one-compound sequencing of oligomer libraries by tandem mass spectrometry, J. Comb. Chem. 8 (2006) 417–426.
[36] C. Gibson, G.A.G. Sulyok, D. Hahn, S.L. Goodman, G. Holzemann, H. Kessler, Nonpeptidic alpha vbeta 3 integrin antagonist libraries: on-bead screening and mass spectrometric identification without tagging, Angew. Chem., Int. Ed. 40 (2001) 165–169.
[37] R. Ruijtenbeek, C. Versluis, A.J.R. Heck, F.A.M. Redegeld, F.P. Nijkamp, R.M.J. Liskamp, Characterization of a phosphorylated peptide and peptoid and peptoid–peptide hybrids by mass spectrometry, J. Mass Spectrom. 37 (2002) 47–55.
[38] J.A.W. Kruijtzer, L.J.F. Hofmeyer, W. Heerma, C. Versluis, R.M.J. Liskamp, Solid-phase syntheses of peptoids using Fmoc-protected N-substituted glycines: the synthesis of (retro)peptoids of leu-enkephalin and substance P, Chem. Eur. J. 4 (1998) 1570–1580.
[39] W. Heerma, J.-P.J.L. Boon, C. Versluis, J.A.W. Kruijtzer, L.J.F. Hofmeyer, R.M.J. Liskamp, Comparing mass spectrometric characteristics of peptides and peptoids. 2, J. Mass Spectrom. 32 (1997) 697–704.
[40] W. Heerma, C. Versluis, C.G. de Koster, J.A.W. Kruijtzer, I. Zigrovic, R.M.J. Liskamp, Comparing mass spectrometric characteristics of peptides and peptoids, Rapid Commun. Mass Spectrom. 10 (1996) 459–464.
[41] P. Roepstorff, J. Fohlman, Proposal for a common nomenclature for sequence ions in mass spectra of peptides, Biomed. Mass Spectrom. 11 (1984) 601.
[42] K. Biemann, S.A. Martin, Mass spectrometric determination of the amino acid sequence of peptides and proteins, Mass Spectrom. Rev. 6 (1987) 1–76.

[43] G.M. Figliozzi, R. Goldsmith, S.C. Ng, S.C. Banville, R.N. Zuckermann, Synthesis of N-substituted glycine peptoid libraries, Methods Enzymol. 267 (1996) 437–447.
[44] V. Sabareesh, P. Balaram, Tandem electrospray mass spectrometric studies of proton and sodium ion adducts of neutral peptides with modified N- and C-termini: synthetic model peptides and microheterogeneous peptaibol antibiotics [Erratum to document cited in CA144:391386], Rapid Commun. Mass Spectrom. 21 (2007) 3227.
[45] D. Bensadek, F. Monigatti, J.A.J. Steen, H. Steen, Why b, y's? Sodiation-induced tryptic peptide-like fragmentation of non-tryptic peptides, Int. J. Mass Spectrom. 268 (2007) 181–189.
[46] M. Rozman, S.J. Gaskell, Non-covalent interactions of alkali metal cations with singly charged tryptic peptides, J. Mass Spectrom. 45 (2010) 1409–1415.
[47] G. Tsaprailis, H. Nair, A. Somogyi, V.H. Wysocki, W. Zhong, J.H. Futrell, S.G. Summerfield, S.J. Gaskell, Influence of secondary structure on the fragmentation of protonated peptides, J Am. Chem. Soc. 121 (1999) 5142–5154.
[48] A.R. Dongre, J.L. Jones, A. Somogyi, V.H. Wysocki, Influence of peptide composition, gas-phase basicity, and chemical modification on fragmentation efficiency: evidence for the mobile proton model, J. Am. Chem. Soc. 118 (1996) 8365–8374.
[49] P. Neta, Q.-L. Pu, L. Kilpatrick, X. Yang, S.E. Stein, Dehydration versus deamination of N-terminal glutamine in collision-induced dissociation of protonated peptides, J. Am. Soc. Mass Spectrom. 18 (2007) 27–36.
[50] T. Lin, G.L. Glish, C-terminal peptide sequencing via multistage mass spectrometry, Anal Chem. 70 (1998) 5162–5165.
[51] T. Lin, A.H. Payne, G.L. Glish, Dissociation pathways of alkali-cationized peptides: opportunities for C-terminal peptide sequencing, J. Am. Soc. Mass Spectrom. 12 (2001) 497–504.
[52] V. Sabareesh, P. Balaram, Tandem electrospray mass spectrometric studies of proton and sodium ion adducts of neutral peptides with modified N- and C-termini: synthetic model peptides and microheterogeneous peptaibol antibiotics, Rapid Commun. Mass Spectrom. 20 (2006) 618–628.
[53] L.M. Mallis, D.H. Russell, Fast atom bombardment-tandem mass spectrometry studies of organo-alkali metal ions of small peptides, Anal. Chem. 58 (1986) 1076–1080.
[54] R.P. Grese, R.L. Cerny, M.L. Gross, Metal ion–peptide interactions in the gas phase: a tandem mass spectrometry study of alkali metal cationized peptides, J. Am. Chem. Soc. 111 (1989) 2835–2842.
[55] P.T.M. Kenny, K. Nomoto, R. Orlando, Fragmentation studies of gas-phase complexes between alkali metal ions and a biologically active peptide, achatin-I, Rapid Commun. Mass Spectrom. 11 (1997) 224–227.
[56] L.M. Teesch, J. Adams, Fragmentations of gas-phase complexes between alkali metal ions and peptides: metal ion binding to carbonyl oxygens and other neutral functional groups, J. Am. Chem. Soc. 113 (1991) 812–820.
[57] L.M. Teesch, R.C. Orlando, J. Adams, Location of the alkali metal ion in gas-phase peptide complexes, J. Am. Chem. Soc. 113 (1991) 3668–3675.
[58] W.Y. Feng, S. Gronert, K.A. Fletcher, A. Warres, C.B. Lebrilla, The mechanism of C-terminal fragmentations in alkali metal ion complexes of peptides, Int. J. Mass Spectrom. 222 (2003) 117–134.
[59] R.P. Grese, M.L. Gross, Gas-phase interactions of lithium ions and dipeptides, J. Am. Chem. Soc. 112 (1990) 5098–5104.
[60] D.H. Russell, E.S. McGlohon, L.M. Mallis, Fast-atom bombardment-tandem mass spectrometry studies of organo-alkali-metal ions of small peptides. Competitive interaction of sodium with basic amino acid substituents, Anal. Chem. 60 (1988) 1818–1824.
[61] J.A. Leary, T.D. Williams, G. Bott, Strategy for sequencing peptides as mono- and dilithiated adducts using a hybrid tandem mass spectrometer, Rapid Commun. Mass Spectrom. 3 (1989) 192–196.
[62] J.A. Leary, Z. Zhou, S.A. Ogden, T.D. Williams, Investigations of gas-phase lithium–peptide adducts: tandem mass spectrometry and semiempirical studies, J. Am. Soc. Mass Spectrom. 1 (1990) 473–480.
[63] M.M. Kish, C. Wesdemiotis, G. Ohanessian, The sodium ion affinity of glycylglycine, J. Phys. Chem. B 108 (2004) 3086–3091.
[64] B.A. Cerda, S. Hoyau, G. Ohanessian, C. Wesdemiotis, Na+ binding to cyclic and linear dipeptides. Bond energies, entropies of Na+ complexation, and attachment sites from the dissociation of Na+-bound heterodimers and ab initio calculations, J. Am. Chem. Soc. 120 (1998) 2437–2448.
[65] T. Wyttenbach, J.E. Bushnell, M.T. Bowers, Salt bridge structures in the absence of solvent? The case for the oligoglycines, J. Am. Chem. Soc. 120 (1998) 5098–5103.
[66] M. Kohtani, B.S. Kinnear, M.F. Jarrold, Metal-ion enhanced helicity in the gas phase, J. Am. Chem. Soc. 122 (2000) 12377–12378.
[67] R. Sudha, M. Panda, J. Chandrasekhar, P. Balaram, Structural effects on the formation of proton and alkali metal ion adducts of apolar, neutral peptides: electrospray ionization mass spectrometry and ab initio theoretical studies, Chem. Eur. J. 8 (2002) 4980–4991.